

# Molecular structure of the glibenclamide binding site of the $\beta$ -cell $K_{ATP}$ channel

Michael V. Mikhailov\*, Ellina A. Mikhailova, Stephen J.H. Ashcroft

*Nuffield Department of Clinical Laboratory Sciences, John Radcliffe Hospital, Headington, Oxford OX3 9DU, UK*

Received 12 March 2001; revised 15 April 2001; accepted 15 May 2001

First published online 31 May 2001

Edited by Gianni Cesareni

**Abstract** We have investigated the structure of the glibenclamide binding site of pancreatic  $\beta$ -cell ATP-sensitive potassium ( $K_{ATP}$ ) channels.  $K_{ATP}$  channels are a complex of four pore-forming Kir6.2 subunits and four sulfonylurea receptor (SUR1) subunits. SUR1 (ABCC8) belongs to the ATP binding cassette family of proteins and has two nucleotide binding domains (NBD1 and NBD2) and 17 putative transmembrane (TM) sequences. Co-expression in a baculovirus expression system of two parts of SUR1 between NBD1 and TM12 leads to restoration of glibenclamide binding activity, whereas expression of either individual N- or C-terminal part alone gave no glibenclamide binding activity, confirming a bivalent structure of the glibenclamide binding site. By using N-terminally truncated recombinant proteins we have shown that CL3 – the cytosolic loop between TM5 and TM6 – plays a key role in formation of the N-terminal component of the glibenclamide binding site. Analysis of deletion variants of the C-terminal part of SUR1 showed that CL8 – the cytosolic loop between TM15 and TM16 – is the only determinant for the C-terminal component of the glibenclamide binding site. We suggest that in SUR1 in the native  $K_{ATP}$  channel close proximity of CL3 and CL8 leads to formation of the glibenclamide binding site. © 2001 Published by Elsevier Science B.V. on behalf of the Federation of European Biochemical Societies.

**Key words:** Potassium channel; Sulfonylurea receptor; Baculovirus; ATP binding cassette protein; SUR1/ABCC8

## 1. Introduction

The pancreatic  $\beta$ -cell ATP-sensitive potassium ( $K_{ATP}$ ) channel [1] couples changes in plasma glucose concentration to insulin secretion [2]. The  $K_{ATP}$  channel is also the site of action of the sulfonylurea drugs used to treat type 2 diabetes, and also of diazoxide, which inhibits insulin secretion and is used to treat insulinoma and neonatal hyperinsulinemia [3,4]. Regulation of  $K_{ATP}$  channels in response to an elevation of blood glucose occurs via increased metabolism of the sugar within the  $\beta$ -cell and a consequent rise in intracellular [ATP]/[ADP] ratio [5]. Closure of  $K_{ATP}$  channels in response to sulfonylureas and opening of the channels by diazoxide involve direct binding of the drugs to the channel [6].

The  $\beta$ -cell  $K_{ATP}$  channel contains two subunits, Kir6.2, an inwardly rectifying K-channel which forms the pore, and SUR1 which contains the binding sites for sulfonylureas and diazoxide and functions as a channel regulator [7–9]. There is evidence for an octameric structure with the active channel containing four molecules each of Kir6.2 and SUR1 [10,11]. Kir6.2 mediates the inhibitory effect of ATP on channel activity [12,13] while SUR1 is responsible for the stimulatory effect of MgADP and K-channel openers [14] and inhibition by sulfonylureas [15]. Hydropathy plots and comparison with related members of the ATP binding cassette (ABC) protein family suggest that SUR1 contains an N-terminal hydrophobic region (TMD0) containing five transmembrane (TM) helices, and two repeats of six TM helices (TMD1 and TMD2); TMD1 and TMD2 are both followed by large cytosolic loops [16]. SUR1 is a member of the ABC superfamily and there is evidence that the two large cytosolic loops, which each contain a Walker A and Walker B motif [17], are nucleotide binding domains (NBDs) [18–20].

Several studies have investigated the regions of Kir6.2 and SUR1 which interact to form the native regulated channel. There is evidence from photoaffinity labelling [10] and immunoprecipitation [21] for close association between Kir6.2 and SUR1. The C-terminus of Kir6.2 has been shown to be involved in interaction with SUR1 [22] and the first TM sequence and the N-terminal region have been implicated in channel assembly [23]. Both N- and C-termini of Kir6.2 cooperate to form the ATP binding site [24]. The cytosolic loop (CL8) between TMs 15 and 16 of SUR1 has been implicated in glibenclamide binding [25,26]. Two distinct regions of TMD2 – part of the cytosolic loops between TM13/TM14 and TMD16/17 – have been implicated in binding K-channel openers [27].

We have previously shown functional expression of  $K_{ATP}$  channels in *Spodoptera frugiperda* insect cells using baculovirus [28]. The properties of the  $K_{ATP}$  channels expressed in insect cells did not differ significantly from those of the native  $\beta$ -cell channel. However, the baculovirus expression system has the advantage that SUR1 and Kir6.2 can be expressed individually at the cell membrane, unlike mammalian cells in which co-expression of both proteins is required for efficient targeting [9,29,30]. We have also shown that when SUR1 is divided in two co-expression in the baculovirus system of the two individual half-molecules leads to expression of glibenclamide binding activity, whereas expression of either individual N- or C-terminal half-molecule shows no glibenclamide binding activity [26]. These observations confirmed the involvement of two separate regions of SUR1 in formation of

\*Corresponding author. Fax: (44)-1865-221834.  
E-mail: michail.mikhailov@ndcls.ox.ac.uk

the glibenclamide binding site. In the present study we have examined which structural fragments of SUR1 are required for glibenclamide binding. We propose a model for the structural organisation of the glibenclamide binding site of SUR1.

## 2. Materials and methods

### 2.1. Cells and viruses

*S. frugiperda* (Sf21) cells and baculoviruses were maintained as previously described [26,28].

### 2.2. Construction of plasmid DNAs and recombinant baculoviruses

Construction of transfer vectors pAcSUR1H, pAcNSUR2 and pAcCSUR2 containing DNA fragments encoding rat SUR1 [7] under control of the polyhedrin promoter in the pAcYM1 vector and corresponding baculoviruses was previously described [1]. pAcNSUR21 and pAcNSUR22 transfer vectors were obtained by cloning in pAcYM1 a PCR copy of SUR1 corresponding to amino acid (aa) sequences 207–984 and 295–984 respectively. Both transfer vectors contain after the coding region a *Bam*HI site and sequence encoding 6×His. PCR copies of the *gfp* gene were cloned in the *Bam*HI sites of pAcNSUR21 and pAcNSUR22 to construct pAcNSUR21G and pAcNSUR22G respectively. pAcSUR1tr, pAcSUR1-17, pAcSUR1-16 and pAcSUR1-16a transfer vectors were obtained by cloning in pAcCasI PCR copies of SUR1 corresponding to aa sequences 55–1299, 55–1274, 55–1246 and 55–1182 respectively (pAcCasI contains the portion of the SUR1 gene encoding aa 1–55, a multicloning site and a His<sub>6</sub> tag [1]). pAcCSUR3tr, pAcCSUR3-17, pAcCSUR3-16 and pAcCSUR3atr transfer vectors were obtained by cloning in pAcYM1 PCR copies of SUR1 corresponding to aa sequences 1093–1299, 1093–1274, 1093–1246 and 1135–1299 respectively and a His<sub>6</sub> tag. pAcSURtr1 and pAcSURtr2 transfer vectors were obtained by cloning in pAcYM1 a PCR copy of SUR1 corresponding to aa sequences 207–1299 and 295–1299 respectively. Deletion variants of pAcSURtr1 transfer vector were obtained by cloning corresponding PCR products in pAcYM1. The resulting pAcSURtr1Δ6/7, pAcSURtr1Δ7/8, pAcSURtr1Δ8/9, pAcSURtr1Δ9/10, pAcSURtr1Δ10/11 transfer vectors have deletions corresponding to aa 295–397, 335–457, 398–526, 458–553, 527–629 respectively. PCR products were obtained by fusion PCR and contained a sequence encoding spacer Ser-Ala-Ser-Ala-Ser-Ala instead of the deleted region. All PCR products contain a sequence encoding a His<sub>6</sub> tag at the 3'-end. The same procedure was used for constructing pAcNSUR21Δ9/10 transfer vector (aa 207–1125 with deletion of aa 458–553). Transfer vectors were used for co-transfection of Sf9 cells together with *Autographa californica* nuclear polyhedrosis virus DNA (AcNPV PAK6) [23]. Recombinant baculoviruses AcNPVNSUR21, AcNPVNSUR22, AcNPVNSUR21G, AcNPVNSUR22G, AcNPVNSUR21Δ9/10, AcNPVNSUR1tr, AcNPVSUR1-17, AcNPVSUR1-16, AcNPVSUR1-17, AcNPVSUR1-16, AcNPVSUR1tr1, AcNPVSUR1tr2, AcNPVSUR1tr1Δ6/7, AcNPVSUR1tr1Δ7/8, AcNPVSUR1tr1Δ8/9, AcNPVSUR1tr1Δ9/10, AcNPVSUR1tr1Δ10/11 were obtained from the corresponding transfer vectors, three times plaque-purified and used for infection of Sf21 cells.

### 2.3. [<sup>3</sup>H]Glibenclamide binding

Sf21 cells resuspended at a density of  $5 \times 10^5$  cells/ml in TC100 were incubated at room temperature (RT) for 30 min with different concentrations of [<sup>3</sup>H]glibenclamide (0.2–10 nM) in a final volume of 400 μl. The incubation was stopped by rapid separation on Whatman GF/C filters soaked in phosphate-buffered saline (PBS) for 30 min beforehand. After washing the filters, specific binding was determined and the dissociation constant,  $K_d$ , and the number of glibenclamide binding sites per cell ( $B_{max}$ ) were estimated as previously described [31].

### 2.4. SDS-PAGE and immunoblotting

SDS-PAGE and immunoblotting were performed as previously described [25]. Anti-His<sub>6</sub> tag antibodies (Penta-His, Qiagen) and alkaline phosphatase conjugated with anti-mouse antibody were used for detection of His-tagged proteins. Rabbit polyclonal anti-NBD1 antiserum (dilution 1:200 000) and alkaline phosphatase conjugated with anti-rabbit antibody were used for detection of recombinant proteins that contained NBD1. Anti-NBD1 antisera were obtained after immunisation of rabbits with purified NBD1 expressed in *Escherichia coli* [1].

### 2.5. Fluorescence microscopy

Insect cells expressing green fluorescent protein (GFP) were grown on cover slips and viewed with a Leitz DMIRB fluorescent microscope (Leica Microscopie und Systeme GmbH). Ionvision III software was used for analysing images.

## 3. Results

### 3.1. Generation of recombinant proteins

Fig. 1 illustrates the predicted topology of SUR1 and the regions of SUR1 expressed by vectors used in this study. The NH<sub>2</sub>-proximal half-molecule designated NSUR2, which contains the first two sets of putative TM domains (TMD0 and TMD1) plus NBD1, was described before [26]. For the present study we constructed truncated NH<sub>2</sub>-proximal half-molecules in which TMD0 (NSUR21) or TMD0 together with the cytosolic loop (CL3) between TMD0 and TMD1 (NSUR22) were deleted. Both NSUR21 and NSUR22 contain no artificial leader sequences. It was therefore essential to establish that these variants were inserted into the plasma membrane. For this purpose we produced variants of both these proteins containing GFP at the COOH end (NSUR21G and NSUR22G). A deletion variant of NSUR21 – NSUR21Δ9/10 – without TM9 and TM10 was also constructed. We also constructed further truncated and deleted variants of SUR1. Since we have previously shown that deletion of the second NBD (NBD2) has no significant effect on glibenclamide binding [26], NBD2 was omitted from constructs described below. We produced three truncated SUR1 constructs: SUR1tr – containing intact NH<sub>2</sub> end of SUR1; SUR1tr1 – with deletion of TMD0; and SUR1tr2 where TMD0 was deleted together with the cytosolic loop (CL3) between TMD0 and TMD1. Deletion variants of SUR1tr1 were also produced. These recombinant proteins contained the spacer sequence Ser-Ala-Ser-Ala-Ser-Ala instead of the two deleted TM domains. Five possible mutants with deletion of two adjacent TM domains from TMD1 were obtained – SUR1tr1Δ6/7, SUR1tr1Δ7/8, SUR1tr1Δ8/9, SUR1tr1Δ9/10, SUR1tr1Δ10/11, with deletion of TM6/TM7, TM7/TM8, TM8/TM9, TM9/TM10, TM10/TM11 respectively. All recombinant proteins were designed to contain a His<sub>6</sub> tag that, as we have shown previously [31], does not interfere with SUR1 assembly and function. Recombinant proteins described above contain NBD1 and we therefore used rabbit polyclonal anti-NBD1 antibodies for detection. Fig. 2 shows Western blots of Sf21 insect cells expressing the recombinant proteins. The positions of the main bands on the Western blot correspond to those predicted from aa sequences.

COOH-proximal half-molecules designated CSUR2 (which contains the last six putative TM helices (TMD2) plus NBD2) and CSUR3 (which contains cytoplasmic loop CL7, the last four putative TM helices from TMD2 plus NBD2) were described before [26]. Further deletion variants of CSUR3 were produced for the present study: CSUR3tr – with deletion of NBD2; CSUR3-17 – with deletion of NBD2 and TM17; CSUR3-16 – with deletion of NBD2, TM16 and TM17; CSUR3atr – with deletion of CL7 and NBD2. All recombinant proteins were designed to contain a His<sub>6</sub> tag and were detected by Western blot with anti-His<sub>6</sub> tag antibodies (data not shown). We also made similar deletions of the whole SUR1 molecule in order to distinguish effects originating from disturbing molecular assembly and those resulting

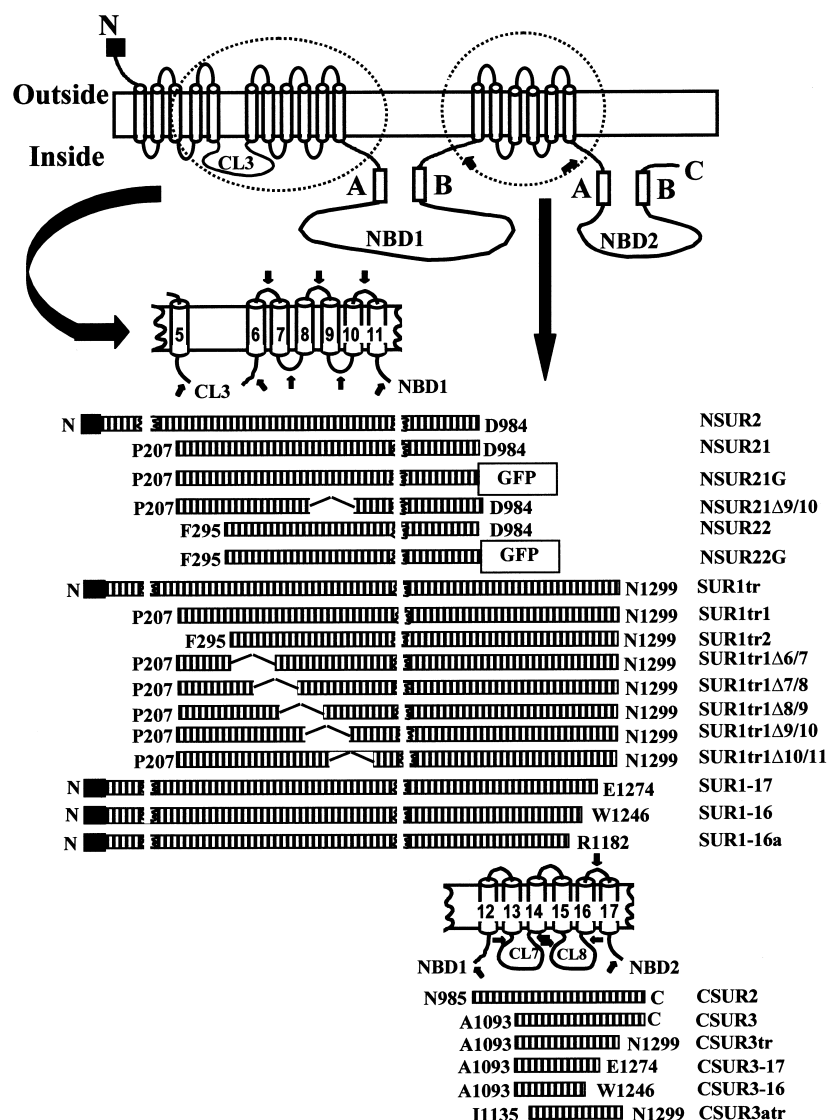


Fig. 1. Predicted topology of SUR1 and design of the recombinant proteins containing regions of SUR1 used in this study. Membrane topologies are based on [16]. Black boxes indicate the SUR1 leader sequence. Stippled lines show SUR1 sequences used in the recombinant proteins whose names are indicated on the right. Arrows indicate sites on SUR1 used for generation of a SUR1 deletion mutant. White boxes (A and B) show the location of Walker A and B motifs that can form nucleotide binding sites in each putative cytosolic NBD (NBD1 and NBD2). The identities and positions in intact SUR1 of the N- and C-terminal aa of each fragment are indicated. All constructs contain a C-terminal His<sub>6</sub> tag.

from destruction of the glibenclamide binding site: SUR1-17 – with deletion of NBD2 and TM17; SUR1-16 – with deletion of NBD2; TM16 and TM17; and SUR1-16a – with deletion of CL8, TM16, TM17 and NBD2.

### 3.2. Expression at the plasma membrane of SUR1 half-molecules

Since neither NSUR21 nor NSUR22 contains an artificial leader sequence we produced variants of these proteins containing GFP at the COOH end (NSUR21G and NSUR22G) to prove plasma membrane localisation of the corresponding proteins. GFP was used as marker for investigation of recombinant protein localisation. Fluorescence microscopy of Sf9 cells expressing recombinant proteins is shown in Fig. 3. GFP itself (Fig. 3A) was randomly distributed inside the insect cell and did not bind to the plasma membrane. Fig. 3B,C shows that NBD21G as well as NBD22G were both expressed

at the plasma membrane of Sf9 insect cells infected with the corresponding recombinant baculovirus. These data show that even without leader sequence truncated variants of SUR1 possess plasma membrane insertion abilities.

### 3.3. Glibenclamide binding to insect cells expressing K<sub>ATP</sub> channel recombinant proteins

In order to characterise glibenclamide binding of different recombinant proteins we measured glibenclamide binding activity at different concentrations of glibenclamide and estimated the binding affinity,  $K_d$  and number of glibenclamide binding sites,  $B_{max}$ . Estimated binding constants and number of binding sites per cell are shown in Table 1. It can be seen that despite varying values of  $B_{max}$ , there are no significant differences in  $K_d$  between different expressed proteins. All binding constants are in the range 1.22–1.92 nM, similar to that for binding of glibenclamide to intact SUR1, 1.81 nM

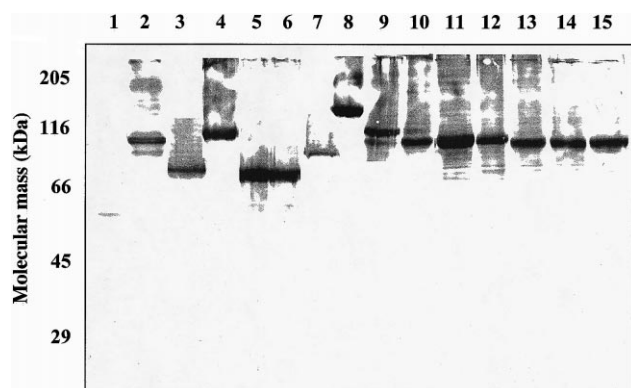


Fig. 2. Western blot of lysed *S. frugiperda* insect cells expressing SUR1 fragments with anti-NBD1 antisera. Lanes: 1 – mock-infected cells; 2 – NSUR2; 3 – NSUR21; 4 – NSUR21G; 5 – NSUR21Δ9/10; 6 – NSUR22; 7 – NSUR22G; 8 – SUR1tr; 9 – SUR1tr1; 10 – SUR1tr2; 11 – SUR1tr1Δ6/7; 12 – SUR1tr1Δ7/8; 13 – SUR1tr1Δ8/9; 14 – SUR1tr1Δ9/10; 15 – SUR1tr1Δ10/11.

(line 5). This indicates that the conformation of the glibenclamide binding site in recombinant proteins is similar to its conformation in native SUR1.

Consistent with our previous observations [31], deletion of NBD2 from the COOH-terminus of SUR1 (SUR1tr) had no significant effect on glibenclamide binding (Table 1, line 6). Further deletion of five TM domains of TMD0 from the NH<sub>2</sub>-terminus of SUR1tr (SUR1tr1) also had no significant effect on glibenclamide binding (Table 1, line 7) whereas deletion of cytosolic loop CL3 between TMD0 and TMD1 (SUR1tr2) abolished binding (Table 1, line 8). This finding indicates a significant role for CL3 in glibenclamide binding.

Investigation of glibenclamide binding with variants of SUR1tr1 with two deleted adjacent TM domains from TMD1 showed that only in the case of deletion of TM9 and TM10 (SUR1tr1Δ9/10; Table 1, line 12) significant binding was retained. This finding indicates that deletion of TM9 and TM10 does not significantly change the conformation of SUR1 and the cytosolic loop between these domains is thus not essential for glibenclamide binding. Other deletion mutants used in the present study (SUR1tr1Δ6/7 with deletion of TM6 and TM7 (Table 1, line 9), SUR1tr1Δ7/8 with deletion of TM7 and TM8 (Table 1, line 10), SUR1tr1Δ8/9 with deletion of TM8 and TM9 (Table 1, line 11) and SUR1tr1Δ10/11 with deletion of TM10 and TM11 (Table 1, line 13)) retained no significant glibenclamide binding.

Table 1

Glibenclamide binding to insect cells expressed different recombinant proteins

Line	Expressed proteins	$K_d$ (nm)	$B_{max}$ (binding sites/cell $\times 10^3$ )
1	NSUR2+CSUR2	$1.43 \pm 0.51$	$863 \pm 41$
2	NSUR21+CSUR2	$1.92 \pm 0.52$	$546 \pm 43$
3	NSUR22+CSUR2	NB	NB
4	NSUR21Δ9/10+CSUR2	$1.37 \pm 0.32$	$383 \pm 51$
5	SUR1	$1.81 \pm 0.53$	$2990 \pm 95$
6	SUR1tr	$1.22 \pm 0.41$	$2201 \pm 80$
7	SUR1tr1	$1.57 \pm 0.62$	$2070 \pm 260$
8	SUR1tr2	NB	NB
9	SUR1tr1Δ6/7	NB	NB
10	SUR1tr1Δ7/8	NB	NB
11	SUR1tr1Δ8/9	NB	NB
12	SUR1tr1Δ9/10	$1.54 \pm 0.44$	$2129 \pm 235$
13	SUR1tr1Δ10/11	NB	NB
14	SUR1-17	$1.61 \pm 0.43$	$2340 \pm 160$
15	SUR1-16	$1.25 \pm 0.57$	$2580 \pm 190$
16	SUR1-16a	NB	NB
17	NSUR2+CSUR3	$1.38 \pm 0.52$	$253 \pm 41$
18	NSUR2+CSUR3tr	$1.83 \pm 0.57$	$524 \pm 58$
19	NSUR2+CSUR3-17	$1.23 \pm 0.41$	$210 \pm 25$
20	NSUR2+CSUR3-16	NB	NB
21	NSUR2+CSUR3atr	$1.73 \pm 0.64$	$590 \pm 61$

Sf21 cells expressing the recombinant proteins indicated were incubated at RT for 30 min with different concentrations of [<sup>3</sup>H]glibenclamide (0.2–10 nM). The incubation was stopped by rapid separation on Whatman GF/C filters soaked in PBS for 30 min beforehand. Filters were washed and specific binding determined. The dissociation constant,  $K_d$ , and the number of glibenclamide binding sites per cell ( $B_{max}$ ) were estimated as described in Section 2. NB: no detectable specific binding.

We have previously demonstrated [26,31] that when SUR1 is divided between NBD1 and TM12 and either the N-terminal SUR1 half-molecule (NSUR2), or the C-terminal half-molecule (CSUR2) expressed separately in *S. frugiperda* cells, glibenclamide binding is not significantly greater than in cells infected with parent baculovirus. However, as confirmed here (Table 1, line 1), in cells co-infected with both halves of SUR1 a substantial increase of glibenclamide binding activity is observed. The present study further demonstrates that glibenclamide binding activity is also retained when the C-terminal half-molecule (CSUR2) is co-expressed with an N-terminal SUR1 half-molecule (NSUR21) in which the TMD0 region is deleted from the COOH end (NSUR21+CSUR2, Table 1, line 2). This indicates that TMD0 is not essential either for glibenclamide binding or for self-assembly of SUR1 half-mol-

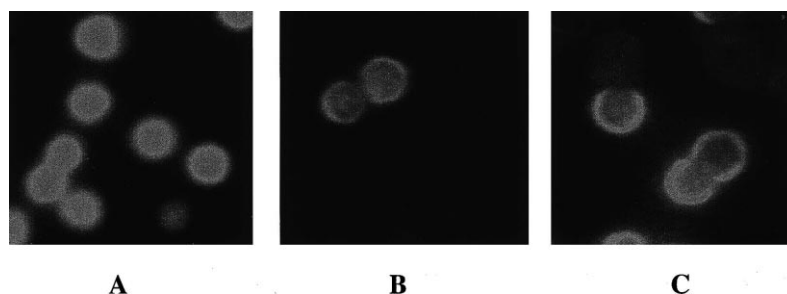


Fig. 3. Fluorescent microscopy of Sf9 insect cells infected with recombinant baculoviruses. Insect cells expressing: A – GFP; B – NSUR21G; C – NSUR22G.

ecules. Further deletion of the cytosolic loop (CL3) between TMD0 and TMD1 from NSUR21 (NSUR22) resulted in loss of glibenclamide binding activity when NSUR22 was co-expressed with CSUR2 (Table 1, line 3), confirming an essential role for CL3 in glibenclamide binding. The deletion variant of NSUR21 where TM9 and TM10 were removed (NSUR21 $\Delta$ 9/10) demonstrated significant glibenclamide binding when co-expressed with CSUR2 (Table 1, line 4). This finding is consistent with the tolerance of SUR1 conformation to such a mutation, as demonstrated above, and confirms that TM9 and TM10 do not take part in self-assembly of SUR1 half-molecules.

As mentioned above, deletion of NBD2 from the COOH-terminus of SUR1 (SUR1tr) had no significant effect on glibenclamide binding (Table 1, line 6). Further deletion of TM17 (SUR1-17, Table 1, line 14) or TM17 and TM16

(SUR1-16, Table 1, line 15) had no significant effect on glibenclamide binding, whereas further deletion of CL8 from the COOH-terminus of SUR1 (SUR1-16a, Table 1, line 16) abolished binding. This finding reflects the importance of CL8 for glibenclamide binding.

Investigation of glibenclamide binding after co-expression of NSUR2 with different truncated variants of CSUR3 shows that: (i) deletion of NBD2 from the COOH end leads to some increase of glibenclamide binding activity, which may be due to facilitated folding (CSUR3tr, Table 1, line 18); (ii) further deletion of TM17 does not prevent glibenclamide binding (CSUR3-17, Table 1, line 19); (iii) further deletion of TM16 abolishes binding (CSUR3-16, Table 1, line 20). Taking into account that deletion from the whole SUR1 molecule of either TM17 or TM16 and TM17 together had no significant influence on glibenclamide binding, we conclude that TM16 is

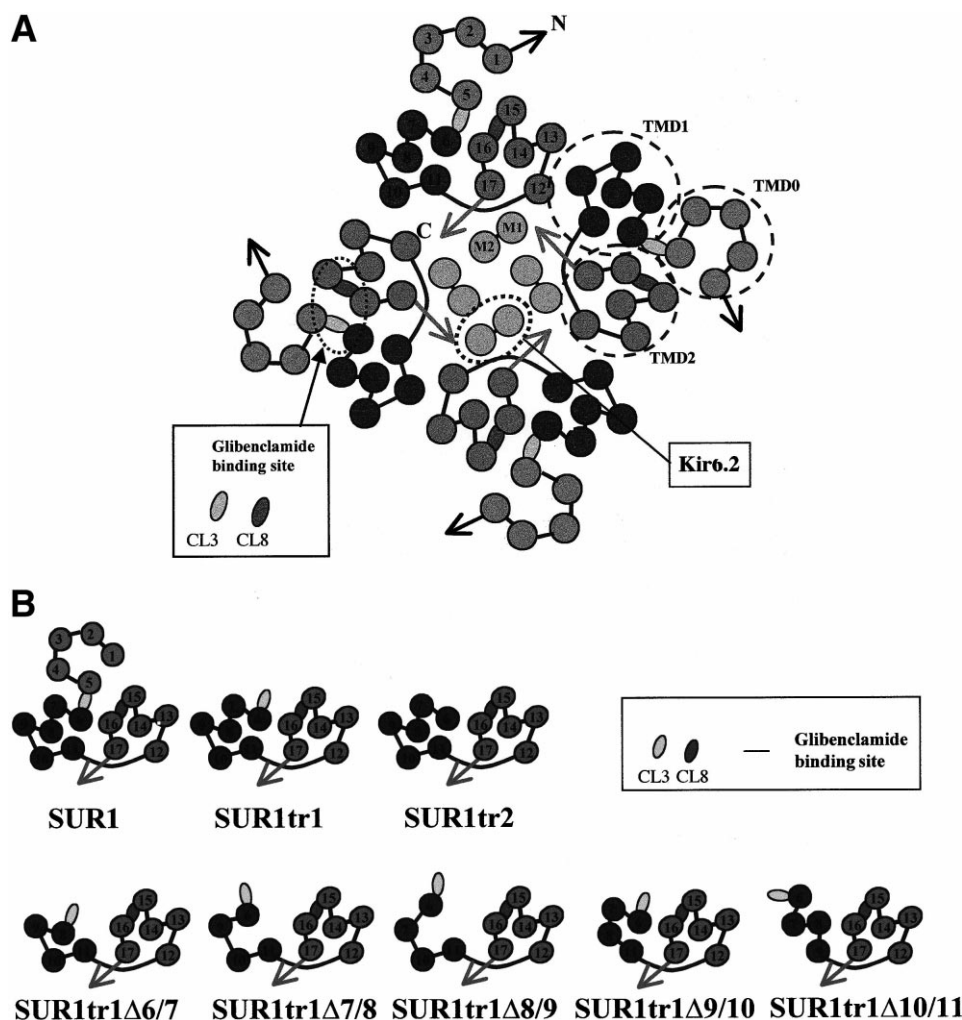


Fig. 4. A: Model of the  $\beta$ -cell  $K_{ATP}$  channel. The figure shows a cross-sectional view of the TM topology of the  $\beta$ -cell  $K_{ATP}$  channel. The current model is based on our previously published model of the  $\beta$ -cell  $K_{ATP}$  channel [31]. Additional features of the model based on the present study are: (i) TMD0 is not essential for assembly; (ii) deletion of TM9 and TM10 does not affect assembly; (iii) TM16 is essential for self-assembly of part molecules. The location of TM sequences in the model also reflects TM12–Kir6.2 interaction and the finding that TM12 and TM13 are not essential for self-assembly [31]. The model indicates the suggested proximity of cytosolic loops between TM5/TM6 (CL3) and TM15/TM16 (CL8), that together form the glibenclamide binding site. The model also shows the presumed internal location of Kir6.2 to form the permeation pathway. B: Model of the truncated and deleted variants of SUR1. The figure provides cross-sectional views within the membrane and illustrates how formation of the glibenclamide binding site could be affected by (i) truncation of SUR1; and (ii) deletion of pairs of TM sequences in TMD1 which alters the distance between CL3 and CL8.

essential for molecular assembly of the SUR1 half-molecules. Deletion of the cytosolic loop between TM13 and TM14 (CL7) from the NH<sub>2</sub>-terminus of CSURtr has no significant effect on glibenclamide binding (CSUR3atr, Table 1, line 21), indicating a lack of involvement of CL7 in glibenclamide binding. Combining data from COOH- and NH<sub>2</sub>-termini truncation we can conclude that CL8 is the only cytosolic structure of SUR1 needed for formation of the C-terminal component of the glibenclamide binding site.

#### 4. Discussion

The first set of five TM domains (TMD0) of SUR1 is not present in the majority of ABC proteins and as we show here does not take part either in SUR1 assembly or in formation of the glibenclamide binding site. This is consistent both with our model of K<sub>ATP</sub> channel structure ([31], Fig. 4A) and with that proposed by Schwappach et al. [23].

Previously, by different approaches, it was demonstrated that formation of the SUR1 high affinity glibenclamide binding site needs the presence of two distinct parts of SUR1 [25,26]. The cytosolic loop between TM15 and TM16 (CL8) is now shown here to be the only cytosolic structure of SUR1 taking part in formation of the C-proximal part of the glibenclamide binding site. The presence of only this loop in a C-terminal half-molecule of SUR1 leads to restoration of glibenclamide binding activity after co-expression with an N-terminal half-molecule. Deletion of this loop abolishes glibenclamide binding. This is consistent with previous data that mutation in this loop (Ser to Tyr at position 1238) leads to a marked decrease of glibenclamide affinity [25,31]. Our data now demonstrate a significant role for the cytosolic loop between TMD0 and TMD1 (CL3) in formation of the N-proximal part of the glibenclamide binding site. Deletion of this loop (from Pro207 to Ala294) leads to loss of glibenclamide binding activity.

It is important for our interpretation of the data to exclude the possibility that a failure of SUR1 fragments to target correctly to the plasma membrane accounts for the negative results when we measure glibenclamide binding in our intact cells (Table 1, lines 3, 8–11, 16, 20). However we do not believe that any of these negative data can be attributed to this mechanism for the following reasons. Firstly, we have shown clearly using GFP-tagged proteins that NSUR21 and NSUR22, which lack a native leader sequence, do correctly insert into the plasma membrane. These data taken together with those of line 2 of Table 1 show that NSUR22 and CSUR2 have reached the membrane. Secondly, since SURtr2 has the same 5'-sequence as NSUR22 we believe it is safe to assume membrane targeting for this construct. Thirdly, the deletion variants have the same 5'-sequence as SURtr1 which our data demonstrate to be capable of correctly targeting the membrane and folding (Table 1, line 6), and the deleted sequences do not contain any known targeting signals. Fourthly, SUR1-16a contains the same leader sequence as native SUR1 and therefore should be correctly targeted. Finally, we have confirmed by using a GFP-tagged version that CSUR3-16 correctly targets the plasma membrane (data not shown).

We therefore interpret the findings in terms of the model of the K<sub>ATP</sub> channel shown in Fig. 4. The model suggests (Fig. 4A) that CL3 and CL8 despite their separate location in the

primary structure of SUR1 can be in close proximity in the three-dimensional structure. Deletion of any two of the TM sequences from TMD1 (except TM9 plus TM10) leads to a change in distance between CL3 and CL8 (Fig. 4B) that could explain loss of glibenclamide binding activity in the corresponding recombinant proteins. TM8 and TM11 could be located proximally such that deletion of TM9 and TM10 does not influence glibenclamide binding or SUR1 assembly (Fig. 4B).

**Acknowledgements:** These studies were supported by a grant from Diabetes UK.

#### References

- [1] Ashcroft, S.J.H. (2000) *J. Membr. Biol.* 176, 187–206.
- [2] Ashcroft, F.M., Ashcroft, S.J.H. and Harrison, D.E. (1986) in: *Biophysics of the Pancreatic  $\beta$ -Cell* (Atwater, I. and Rojas, E., Eds.).
- [3] Sturgess, N.C., Kozlowski, R.Z., Carrington, C.A., Hales, C.N. and Ashford, M.L. (1988) *Br. J. Pharmacol.* 95, 83–94.
- [4] Dunne, M.J., Kane, C., Shepherd, R.M., Sanchez, J.A., James, R.F.L., Johnson, P.R.V., Aynsley-Green, A., Lu, S., Clement IV, J.P., Lindley, K.J., Seino, S. and Aguilar-Bryan, L. (1997) *New Engl. J. Med.* 336, 1344–1347.
- [5] Ashcroft, S.J.H. and Ashcroft, F.M. (1990) *Cell. Signal.* 2, 197–214.
- [6] Ashcroft, S.J.H. and Ashcroft, F.M. (1992) *Biochim. Biophys. Acta* 1175, 45–59.
- [7] Sakura, H., Åmmälä, C., Smith, P.A., Gribble, F.M. and Ashcroft, F.M. (1995) *FEBS Lett.* 377, 338–344.
- [8] Aguilar-Bryan, L., Nichols, C.G., Wechsler, S.W., Clement, J.P., Boyd III, A.E., González, G., Herrera-Sosa, H., Nguy, K., Bryan, J. and Nelson, D.A. (1995) *Science* 268, 423–426.
- [9] Inagaki, N., Gono, T., Clement, J.P., Namba, N., Inazawa, J., Gonzalez, G., Aguilar-Bryan, L., Seino, S. and Bryan, J. (1995) *Science* 270, 1166–1170.
- [10] Clement, J.P., Kunjilwar, K., Gonzalez, G., Schwanstecher, M., Panten, U., Aguilar-Bryan, L. and Bryan, J. (1997) *Neuron* 18, 827–838.
- [11] Shyng, S.L. and Nichols, C.G. (1997) *J. Gen. Physiol.* 110, 655–664.
- [12] Tucker, S.J., Gribble, F.M., Zhao, C., Trapp, S. and Ashcroft, F.M. (1997) *Nature* 387, 179–183.
- [13] John, S.A., Monck, J.R., Weiss, J.N. and Ribalet, B. (1998) *J. Physiol.* 510, 333–345.
- [14] Gribble, F.M., Tucker, S.J. and Ashcroft, F.M. (1997) *EMBO J.* 16, 1145–1152.
- [15] Gribble, F.M., Tucker, S.J., Seino, S. and Ashcroft, F.M. (1998) *Diabetes* 47, 1412–1418.
- [16] Tusnady, G.E., Bakos, E., Varadi, A. and Sarkadi, B. (1997) *FEBS Lett.* 402, 1–3.
- [17] Walker, J., Saraste, M., Runswick, M. and Gah, N. (1982) *EMBO J.* 1, 945–951.
- [18] Ueda, K., Komine, J., Matsuo, M., Seino, S. and Amachi, T. (1999) *Proc. Natl. Acad. Sci. USA* 96, 1268–1272.
- [19] Matsuo, M., Kioka, N., Amachi, T. and Ueda, K. (1999) *J. Biol. Chem.* 274, 37479–37482.
- [20] Bienengraeber, M., Alekseev, A.E., Abraham, M.R., Carrasco, A.J., Moreau, C., Vivaudou, M., Dzeja, P.P. and Terzic, A. (2000) *FASEB J.* 14, 1943–1952.
- [21] Lorenz, E., Alekseev, A.E., Krapivinsky, G.B., Carrasco, A.J., Clapham, D.E. and Terzic, A. (1998) *Mol. Cell. Biol.* 18, 1652–1659.
- [22] Glibin, J.P., Leane, J.L. and Tinker, A. (1999) *J. Biol. Chem.* 274, 22652–22659.
- [23] Schwappach, B., Zerangue, N., Jan, Y.N. and Jan, L.Y. (2000) *Neuron* 26, 155–167.
- [24] Tucker, S.J., Gribble, F.M., Proks, P., Trapp, S., Ryder, T.J., Haug, T., Reimann, F. and Ashcroft, F.M. (1998) *EMBO J.* 17, 3290–3296.

- [25] Ashfield, R., Gribble, F.M., Ashcroft, S.J.H. and Ashcroft, F.M. (1999) *Diabetes* 48, 1341–1347.
- [26] Mikhailov, M.V. and Ashcroft, S.J.H. (2000) *J. Biol. Chem.* 275, 3360–3364.
- [27] Uhde, I., Toman, A., Gross, I., Schwanstecher, C. and Schwanstecher, M. (1999) *J. Biol. Chem.* 274, 28079–28082.
- [28] Mikhailov, M.V., Proks, P., Ashcroft, F.M. and Ashcroft, S.J.H. (1998) *FEBS Lett.* 429, 390–394.
- [29] Sakura, H., Bond, C., Warren-Perry, M., Horsley, S., Kearney, L., Tucker, S., Adelman, J., Turner, R. and Ashcroft, F.M. (1995) *FEBS Lett.* 367, 193–197.
- [30] Zerangue, N., Schwappach, B., Jan, Y.N. and Jan, L.Y. (1999) *Neuron* 22, 537–548.
- [31] Mikhailov, M.V., Mikhailova, E.A. and Ashcroft, S.J.H. (2000) *FEBS Lett.* 482, 59–64.